Available online at www.sciencedirect.com

ScienceDirect

journal homepage: www.elsevier.com/locate/he

Chemical bulk diffusion and electrochemical properties of $SmBa_{0.6}Sr_{0.4}Co_2O_{5+\delta}$ cathode for intermediate solid oxide fuel cells

Adi Subardi [a,b], *Meng-Hsien Cheng* [a], *Yen-Pei Fu* [a,c,*]

[a] *Departement of Materials Science & Engineering, National Dong Hwa University, Shou-Feng, Hualien 97401, Taiwan*

[b] *Departement of Mechanical Engineering, STTNAS, Yogyakarta 55281, Indonesia*

[c] *Nanotechnology Research Center, National Dong-Hwa University, Shou-Feng, Hualien 97401, Taiwan*

ARTICLE INFO

Article history:
Received 28 April 2014
Received in revised form
24 June 2014
Accepted 25 June 2014
Available online 2 August 2014

Keywords:
Intermediate temperature solid oxide fuel cells
Electrical conductivity relaxation method
Diffusion coefficient
Exchange current density
Oxygen reduction reaction

ABSTRACT

In this work, the chemical bulk diffusion coefficient (D_{chem}) of $SmBa_{0.6}Sr_{0.4}Co_2O_{5+\delta}$ was determined by an electrical conductivity relaxation (ECR) method. The equation of D_{chem} as a function of temperature in the range of 500–700 °C exhibits as follows:

$D_{chem} = 1.77\times10^{-5}$ (−68.039 (kJ mol^{-1})/RT) (m^{2}s^{-1})

Electrochemical impedance spectroscopy (EIS) technique was performed over the temperature range of 600–850 °C to determine the cathode polarization resistance (R_p). The area specific resistances (ASR) of $SmBa_{0.6}Sr_{0.4}Co_2O_{5+\delta}$-$Ce_{0.8}Sm_{0.2}O_{1.9}$ (70:30 in wt%) composite cathode were 5.16, 0.86 and 0.21 Ω cm^2 at the operating temperatures of 600, 700 and 800 °C respectively. The exchange current densities (i_o) for oxygen reduction reaction (ORR) were determined from the EIS approach, and low-field and high-field cyclic voltammetry. The activation energies (E_a) of ORR determined from the slope of Arrhenius plots for EIS, low-field and high-field technique were 148.6, 69.8 and 74.2 kJ mol^{-1}, respectively. Based on the electrochemical properties, the mixed-ionic-and-electronic conductor (MIEC) of $SmBa_{0.6}Sr_{0.4}Co_2O_{5+\delta}$ is a potential cathode for intermediate temperature solid oxide fuel cells (IT-SOFCs) based on a SDC electrolyte.

Introduction

Solid oxide fuel cells (SOFCs) are advanced electrochemical reactors that convert chemical energy directly into electrical energy. Lowering their operating temperature to around 600–800 °C is one of the main goals in current SOFC research. The development of cathode materials with high-electrocatalytic activity for oxygen reduction reaction (ORR) at intermediate temperature has received considerable attention during the past decades [1,2]. The cathodic reaction involves the reduction of molecule oxygen to oxygen ion by means of a

* *Corresponding author*. Department of Materials Science & Engineering, National Dong-Hwa University, Shou-Feng, Hualien 97401, Taiwan. Tel.: +886 3 863 4209; fax: +886 3 863 4200.
E-mail address: d887503@alumni.nthu.edu.tw (Y.-P. Fu).

http://dx.doi.org/10.1016/j.ijhydene.2014.06.134

series of intermediate steps, including gas diffusion, surface adsorption, dissociation, charge transfer and so on [3,4]. Consequently, evaluation of the electrocatalytic activity of the cathode shifted toward oxygen reduction at reduced temperature is very important for intermediate temperature solid oxide fuel cells (IT-SOFCs). The detailed information about the surface exchange and oxygen bulk diffusion properties will be helpful in understanding the electrochemical properties of the cathode, as well as in providing further guidance on performance optimization [5].

There are several techniques that can be applied to determine the surface exchange and bulk diffusion coefficients of a mixed conductor, such as oxygen permeation measurements, coulometric titrations, electrochemical impedance spectroscopy, oxygen isotope exchange depth profiling (IEDP) using secondary ion mass spectrometry (SIMS), oxygen isotope exchange using mass spectrometry, and relaxation techniques. The electrical conductivity relaxation (ECR) method has turned out to be a facile way to measure the chemical bulk diffusion coefficient (D_{chem}) of a mixed conductor due to the high sensitivity of electrical conductivity to changes in oxygen concentration or oxygen partial pressure [6–11]. Therefore, the ECR method was used to measure D_{chem} in this research.

A reduced operating temperature can reduce problems with sealing and thermal degradation, allow the use of low-cost metal interconnection materials, and suppress reactions between the cell components, thus lowering the costs of IT-SOFCs. However, the electrochemical activity of the cathode dramatically decreases with decreasing temperature. The cathodes become the limiting factor in determining the overall cell performance. Therefore, the development of the new electrodes with high-electrocatalytic activity for the ORR is critical for IT-SOFCs [12,13]. The high performance cathodes for IT-SOFC mostly based on perovskite structure (ABO_3) and related structures in these days. The cobaltites with excellent electrochemical properties have been reported for IT-SOFC cathode [13–15]. They are known for their excellent mixed-ionic-and-electronic conductor (MIEC) performance in the intermediate temperature range. In the recent years, there have been some reports regarding the remarkable ORR activities in oxygen-deficient layered perovskites in the intermediate temperature range. It is a new class of materials suitable for application as cathodes in IT-SOFCs, which require high oxygen diffusion rates and surface exchange kinetics at intermediate temperatures [14–17].

In typical A-site ordered perovskites, $LnBaCo_2O_{5+\delta}$, oxygen can move easily through the LnO plane, which was observed through neutron diffraction and molecular dynamics simulations [18,19]. In order to enhance the oxygen mobility in the LnO plane, different lanthanides and alkali-earth metals have been tried to dope into the A-site of oxygen-deficient layered perovskites such as $NdBa_{1-x}Sr_xCo_2O_{5+\delta}$ [20] and $YBa_{0.6}Sr_{0.4}Co_2O_{5+\delta}$ [21]. Based on Ref. [21], the Sm was substituted for Y in the present work, the $SmBa_{0.6}Sr_{0.4}Co_2O_{5+\delta}$ cathode characteristics such as the exchange current density (i_o) determined using EIS, low-field (LF) and high-field (HF) technique, and chemical bulk diffusion coefficient (D_{chem}) determined using ECR method were investigated.

Experimental

Cathode and electrolyte materials preparation

The $SmBa_{0.6}Sr_{0.4}Co_2O_{5+\delta}$ (SBSC) cathode powders were prepared by the solid-state reaction. The Sm_2O_3, $SrCO_3$, CoO, and $BaCO_3$ powders were used as starting materials. These powders were mixed under ethanol and milled for 12 h using zirconia balls. The ball-milled mixture was dried and ground into fine powder with mortar and pestle, and then calcined in air at 1100 °C for 6 h. The $Ce_{0.8}Sm_{0.2}O_{1.9}$ (SDC) powder was synthesized by co-precipitation process using $Ce(NO_3)_3{\cdot}6H_2O$, and $Sm(NO_3)_3{\cdot}6H_2O$ as the starting materials. These starting materials were dissolved in distilled water with stoichiometric ratio and then added to ammonia solution (28%). The mixture solution was adjusted to a pH value in the range of 9.5–10. The resulting precipitate was filtered in a vacuum, and washed three times with distilled water and ethanol, respectively. Then the coprecipitation powder was calcined in air at 600 °C for 2 h. The SDC powder samples were pelletized with a small amount of polyvinyl alcohol (PVA) as binder under an applied uniaxial pressure of 1000 kgf/cm^2 to the dimensions of 15 mm in diameter and 1 mm in thick. The disc samples were then finally sintered at 1500 °C for 5 h with a programmed heating rate of 5 °C/min and a cooling rate of 3 °C/min [22].

Electrical conductivity relaxation

The electrical conductivity was measured by the four-probe DC method, where two silver wires acting as current leads and two other silver wires acting as voltage probes were attached to the electrodes. A constant current was delivered to the two current wires, and the voltage response was recorded by an Electrochemical workstation 5000. Measurement was performed on a specimen with a rectangle geometry, having typical size of $5 \times 5 \times 10$ mm^3 and above 95% of the theoretical density over the temperature range of 500–700 °C at an interval of 50 °C. After each temperature change, the bar was stabilized for at least 30 min. A sudden change in the oxygen partial pressure (P_{O_2}), from 0.05 to 0.21 atm was caused by introducing standard gas mixtures of Ar and O_2. Small oxidation and reduction steps were alternatively applied to study the D_{chem}. Typically, a sequence of several reduction/oxidation cycles was performed at each temperature. The electrical conductivity relaxation curve was plotted as $g(t)$ versus t, which was fit by a least square method to an analytical solution of Eq. (1). D_{chem} was the variable fitting parameters [5].

Symmetrical cell fabrication

The composite working electrode (WE) was prepared by the ethanol-based ball mill method. The 70SBSC-30SDC composite cathode consisted of SBSC: SDC (in wt%) = 70:30. The 70SBSC-30SDC composite cathode paste consists of cathode powder, solvent, binder, and plasticizer. The cathode paste was applied by screen-printing on both sides of SDC electrolyte discs in circles of 13 mm diameter and 1 mm thick. On one side, the 70SBSC-30SDC composite cathode paste

was painted as the WE with surface area of 0.385 cm^2. The Ag reference electrode (RE) was placed away from the WE by about 0.3–0.4 cm. Such a distance was chosen to avoid measurement errors due to the misalignment of the working and counter electrodes [23–25]. The Ag counter electrode (CE) was placed on the other side of the SDC disk. After the 70SBSC-30SDC composite cathode material was painted on the electrolyte, it was sintered at 1000 °C for 4 h in air.

Electrochemical and half cell measurement

The symmetrical testing cell experiments were carried out under air ($P_{O_2} = 0.21$ atm) in temperatures ranging from 600 to 850 °C at intervals of 50 °C in a furnace. The AC impedance measurement was performed using the VoltaLab PGZ301 potentionistat with frequency applied range from 100 kHz to 0.1 Hz with 10 mV AC signal amplitude. Under the cathodic polarized condition, the EIS was conducted as a function of the applied cathodic voltage (E). The EIS fitting analysis was performed with the Zview software. Linear sweep voltammetry was measured between −0.4 V and 0.1 V with sweep rate 0.5 mV/s versus the RE.

Material characterization

The structure and phase stability of the sintered cathodes were characterized by X-ray powder diffractometer (XRD; Rigaku D/MAX-2500V), with a scanning rate of 4°/min and scanning range of 10–80°, using a Cu K_α (1.5418 Å) radiation source. The powder pattern and lattice parameter were analyzed by Rietveld refinement using the GSAS program. The morphology of 70SBSC-30SDC composite was observed by scanning electron microscopy (SEM; Hitach 3500H).

Result and discussion

Structure of SBSC

X-ray diffraction patterns of SBSC powders were calcined at different temperatures (900, 1000 and 1100 °C) for 6 h, the characteristic XRD peaks of double-perovskite oxide were detected. The XRD patterns of SBSC were illustrated in Fig. 1(a), it can be seen that the powders are well crystallized. There are not any peaks attributable to impurities in the structure of SBSC as calcining temperature at 1100 °C. However, there are some impurities in SBSC for the specimen sintered at 900 °C and 1000 °C. The XRD pattern show the formation of impurities phase such as $SmCoO_3$ (JCPDS 25-1071), Co_2O_3 (JCPDS 42-1467), Sm_2CoO_4 (JCPDS 72-0938) and $BaCoO_2$ (JCPDS 40-0722). A peak of (102) shifts toward lower angles with increasing the calcining temperatures, which indicates that there is an expansion in unit-cell volume; however, the amount of impurities decreased with increasing the calcining temperatures. Fig. 1(b) shows the refinement of SBSC patterns including the measured XRD data, the calculated profile and the difference between them. Cell parameters regarding SBSC obtained from the Rietveld refinement is listed in Table 1. The experimental data highly agree with the

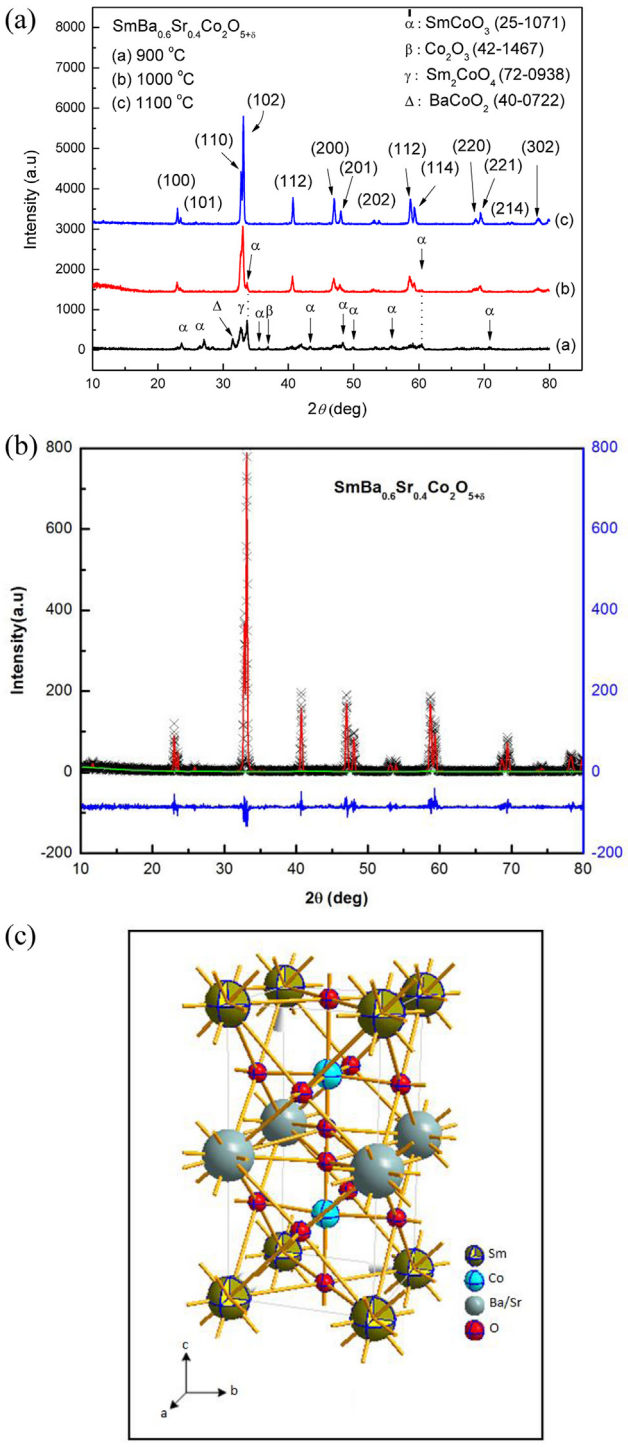

Fig. 1 – (a) X-ray powder diffraction pattern of SBSC calcined between 900 and 1100 °C; (b) Observed (crosses) and calculated (solid line) XRD profiles and the difference (bottom line) between them for SBSC calcined at 1100 °C; (c) Crystal structure of SBSC at room temperature, in which Ba^{2+}/Sr^{2+} ions were in the ordered perovskite lattice.

calculated profiles, suggesting that cations are well ordered in the double-perovskite lattice [26,27] Based on the refinement data, it revealed that the diffraction pattern of SBSC sample is a tetragonal structure (space group: P4/mmm, no. 123) with

Table 1 – Crystal structure of $SmBa_{0.6}Sr_{0.4}Co_2O_{5+\delta}$ cell parameters obtained from the Rietveld refinement.[a]

Atom	Site	x	y	z	Uiso	Occ
SM_1	1a	0	0	0	0.02187	1
CO_2	2h	0.5	0.5	0.25344	0.00741	1
BA_3	1b	0	0	0.5	0.01140	0.6
O_4	4i	0	0.5	0.26778	0.01534	0.9055
O_5	1c	0.5	0.5	0	0.02027	1.0091
O_6	2h	0.5	0.5	0.44106	0.00711	0.457
SR_7	1b	0	0	0.5	0.025	0.4

[a] $R_p = 1.88\%$, $R_{wp} = 2.89\%$, $R_{exp} = 3.337\%$, space group P4/mmm (No. 123)-tetragonal, $a = 3.87$ Å, $b = 3.87$ Å, $c = 7.59$ Å, $v = 114.11$ Å^3.

lattice parameters of $a = 3.87$ Å, $b = 3.87$ Å, $c = 7.59$ Å and $V = 114.11$ Å^3. In SBSC crystal structure, Sm atoms are located at 1a positions, Ba and Sr atoms are distributed at random over the 1b sites. While Co atoms are placed at 2 h positions and oxygen atoms are located at 4 i, 1 c and 2 h sites. A view of the crystal structure of SBSC at room temperature is shown in Fig. 1(c).

Chemical diffusion coefficient (D_{chem})

The electrode performance is closely related to the intrinsic properties of the electrode material such as bulk diffusion and surface exchange kinetics properties. In this study, D_{chem} was measured by an ECR technique, which is based on the principle that a variation in the ambient atmosphere leads to a change in the oxygen vacancy concentration of the MIEC. Due to the local electroneutrality requirement, the abrupt change in the oxygen partial pressure of the surrounding atmosphere induces a corresponding change of the charge carrier concentration (oxygen vacancy), which is reflected as a relaxation of the apparent macroscopic electrical conductivity [28]. This relaxation process is accompanied with oxygen exchange at the surface and chemical diffusion in the bulk of the oxide sample. Conductivity relaxation models usually assume small departures from thermal equilibrium and a simple linear model for the surface exchange kinetics [29]. Fig. 2(a) shows the electrical conductivity relaxation curves of SBSC at various temperatures by a sudden change in the P_{O_2} from 0.21 to 0.05 atm. The elemental steps for the oxygen exchange could be considered as (i) surface reaction which involves ionization of oxygen or deionization of oxide ions at the gas/solid interface and (ii) diffusion in solid specimen. In the solid, movement of oxide ions is counter-balanced by a simultaneous motion of electron holes, which is characterized as a chemical diffusion process.

The values for D_{chem} could be obtained by fitting the electrical conductivity relaxation curves into Eq. (1). SBSC cathode in the reduction process was given in Table 2.

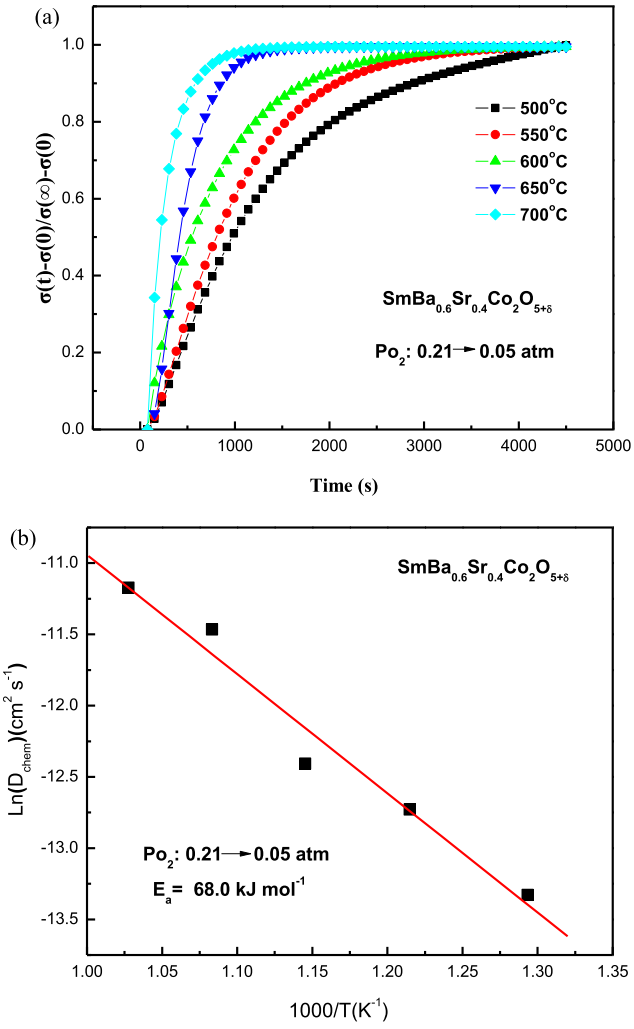

Fig. 2 – (a) The electrical conductivity relaxation curves for SBSC at various temperatures after the oxygen pressure suddenly changed from 0.21 to 0.05 atm; (b) Arrhenius plots of D_{chem} vs. 1000/*T* for SBSC cathode between 500 and 700 °C.

where D_{chem} is the chemical diffusion coefficient, and $\sigma(0)$, $\sigma(t)$ and $\sigma(\infty)$ indicated the initial, time dependent and final conductivities, respectively. The coefficients of α_{1n}, α_{2m} and α_{3p} are the *n*th, *m*th and *p*th roots of the transcendental equations:

$$C_1 = \alpha_{1n}\tan\alpha_1,\ C_2 = \alpha_{2m},\ C_3 = \alpha_{3p}\tan\delta_{3p} \quad (2)$$

The parameter of C_1, C_2 and C_3 are defined as:

$$C_1 = 1_1/L_d,\ C_2 = L_2/L_d,\ C_3 = D_{chem}/k_{ex} \quad (3)$$

$$\frac{\alpha(t)-\sigma(0)}{\sigma(\infty)-\sigma(0)} = 1 - \sum_{n=1}^{\infty}\sum_{m=1}^{\infty}\sum_{p=1}^{\infty} x\frac{2C_1^2\exp\left(-\alpha_{1n}^2 D_{chem}t/l_1^2\right)}{\alpha_{1n}^2(\alpha_{1n}^2+\alpha_1^2+C_1)} x\frac{2C_2^2\exp\left(-\alpha_{2m}^2 D_{chem}t/l_2^2\right)}{\alpha_{2m}^2(\alpha_{2m}^2+C_3^2+C_2)} x\frac{2C_3^2\exp\left(-\alpha_{3p}^2 D_{chem}t/l_3^2\right)}{\alpha_{3p}^2\left(\alpha_{3p}^2+C_3^2+C_3\right)} \quad (1)$$

Table 2 – D_{chem} of $SmBa_{0.6}Sr_{0.4}Co_2O_{5+\delta}$ at various temperatures from electrical conductivity relaxation curves during the oxygen partial pressure suddenly changed from 0.21 to 0.05 atm.

Temperature (°C)	D_{chem} (cm^2s^{-1})
500	1.63×10^{-6}
550	2.96×10^{-6}
600	4.09×10^{-6}
650	1.05×10^{-5}
700	1.41×10^{-5}

where k_{chem} is the surface exchange coefficient in the relaxation process. The conductivity reached its steady state value faster at the high temperatures than the low temperatures, leading to the fact that D_{chem} at high temperatures was larger than one at low temperatures. D_{chem} values of SBSC measured via ECR technique are 1.63×10^{-6}, 4.09×10^{-6} and 1.41×10^{-5} cm^2 s^{-1} at 500, 600 and 700 °C, respectively. The activation energy for D_{chem} obtained from the slope of Arrhenius plot as shown in Fig. 2(b) was 68.0 kJ mol^{-1}. The activation energy for $SmBa_{0.6}Sr_{0.4}Co_2O_{5+\delta}$ is less than that of $Ba_{0.5}Sr_{0.5}Co_{0.8}Fe_{0.2}O_{3-\delta}$ of 111 kJ mol^{-1} [5]. The equation of D_{chem} as a function of temperature in the range of 500–700 °C range of exhibits as follow:

$$D_{chem} = 1.77 \times 10^{-5}\left(-\frac{68.03(\text{kJ mol}^{-1})}{RT}\right)(\text{m}^2\text{s}^{-1}) \quad (4)$$

Interfacial polarization resistance

Cathode performance was investigated by the AC impedance spectroscopy based on a symmetrical 70SBSC-30SDC composite cathode on SDC electrolyte testing cell, recorded under open-circuit conditions. Polarization resistance of the 70SBSC-30SDC composite cathode was measured directly from the difference between high-and low-frequency intercepts on the real axis of the impedance plot [30]. Fig. 3(a) shows the impedance spectra measured under open-circuit conditions over the temperature range of 600–850 °C in air. An equivalent circuit of the impedance curve was used to illustrate the resistance of the testing cell and was fitted well by the model R_1 (R_2–CPE_1) (R_3–CPE_2). The R_1 is equivalent to Ohmic resistance (R_Ω), and the polarization resistance (R_p) is defined by two resistances ($R_2 + R_3$). A constant phase element (CPE) represents a nonideal capacitor, e.g., of the double layer at a nonplanar TPB, and the associated n parameter indicates the CPE's similarity to a true capacitor, for which n is 1. The CPE values are obtained by fitting experimental data to Eq. (5) [31].

$$Z = \frac{1}{\text{CPE}(j\omega)^n} \quad (5)$$

The high-frequency intercept of the impedance spectrum gives the Ohmic resistance of the cell (R_Ω), including the resistance contributions of the electrolyte, the two electrodes, the current collectors and the lead wires. The total cathode polarization resistance (R_p) includes the effective interfacial polarization resistance corresponding to the electrochemical reactions at the electrode-electrolyte interface (R_2) and concentration polarization (mass-transfer or gas diffusion polarization) resistance (R_3). The resistance at the high-frequency is probably associated with charge transfer processes (R_2), including the electron transfer and ion transfer processes occurring at the current collector/cathode electrode and the cathode electrode/electrolyte interfaces, respectively. The low-frequency arc can be attributed to the diffusion processes (R_3), which include adsorption-desorption of oxygen, oxygen diffusion at the gas-cathode surface interface and surface diffusion of intermediate oxygen species [32–34].

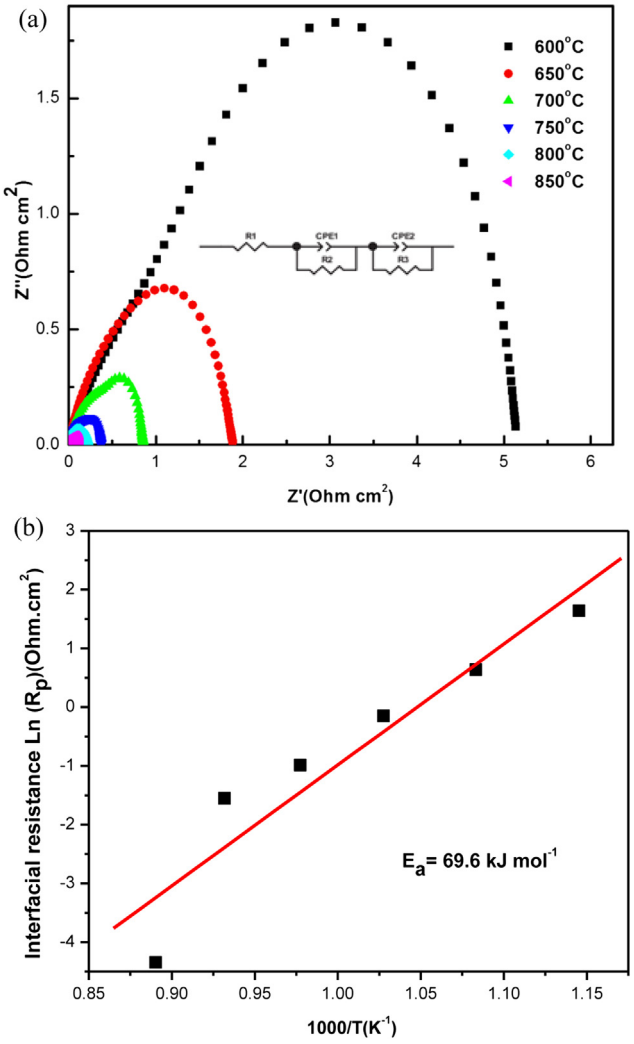

Fig. 3 – (a) Nyquist plots of EIS over the temperature range of 600–850 °C and (b) Total interfacial polarization resistance (R_p) for 70SBSC-30SDC composite cathode.

In this study, the cathode polarization resistance was represented by area specific resistance (ASR). The total cathode polarization resistance (R_p) decreased dramatically with increasing temperature, and the values of R_p were 5.16, 0.86, and 0.21 Ω cm^2 at 600, 700, and 800 °C, respectively for 70SBSC-30SDC composite cathode. The activation energies (E_a) of cathode polarization resistance was 69.6 mol^{-1} (Fig. 3(b)), this value is lower than the SBSCF–SDC (93.7 kJ mol^{-1}) composite cathode reported in Ref. [35]. This suggests that the 70SBSC-30SDC composite cathode with a continuous and three dimensional frameworks provided the

gas a pathway for easier transport, thereby reducing in the activation energy of cathode polarization resistance. Fig. 4 shows the SEM image of top-view morphology of 70SBSC-30SDC composite cathode, which revealed the uniform grain sizes distributed in the range of 1–2 μm and was porous. Such a good morphology is helpful to guarantee a fast diffusion of oxygen and reduces the polarization resistance and enhances the current collection.

The exchange current density (i_o)

The i_o value is an important parameter for assessing the intrinsic oxygen reduction rate and evaluating the electrochemical properties of cathode [36]. The i_o values can be obtained via different measuring techniques. In the present work, the i_o values were determined using EIS, LF and HF technique. For EIS technique, i_o values were measured from the R_p of the Nyquist plot and calculated using Eq. (6), which is derived from the Butler Volmer equation [37]:

$$i_o = \frac{RT\nu}{nFR_p} \tag{6}$$

Here, n is the total number of electrons passed in the reaction, ν reflects the number of times the rate-determining step occurs for one occurrence of the full reaction, F is the Faraday constant (F = 96,500 C/mol), and R is the ideal gas constant (R = 8.31 J/mol K). For the ORR, n and ν are generally assumed to be 4 and 1 respectively, since the total number of electrons transferred per molecule of oxygen reduced is 4 and the rate limiting step would likely have a stoichiometry of 1 for the oxygen reduction reaction [38].

For LF technique, i_o values were determined from the slope of the i vs. η plots as shown Fig. 5(a). The calculation of i_o values was based on Eq. (7). The slopes were determined within potential range of ±30.1, 31.8, 33.5, 35.3, 37.1 and 38.7 mV for 600, 650, 700, 750, 800 and 850 °C, respectively.

$$i_o = \frac{RT\nu}{nF}\text{slope} \tag{7}$$

For HF technique, i_o values can be obtained from the y-intercept of i vs. η plots as shown in Fig. 5(b) based on Eq. (8).

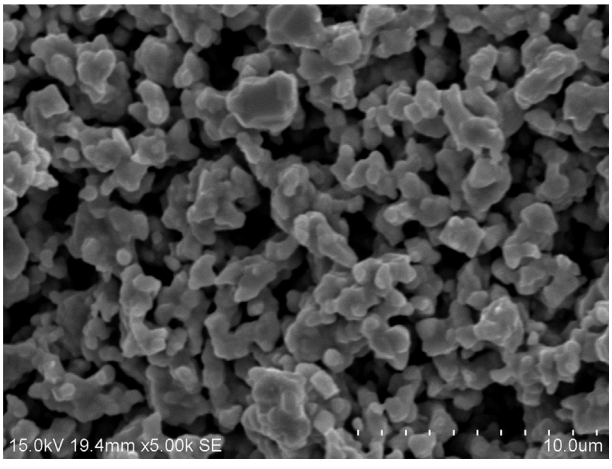

Fig. 4 – SEM morphology of 70SBSC-30SDC composite cathode.

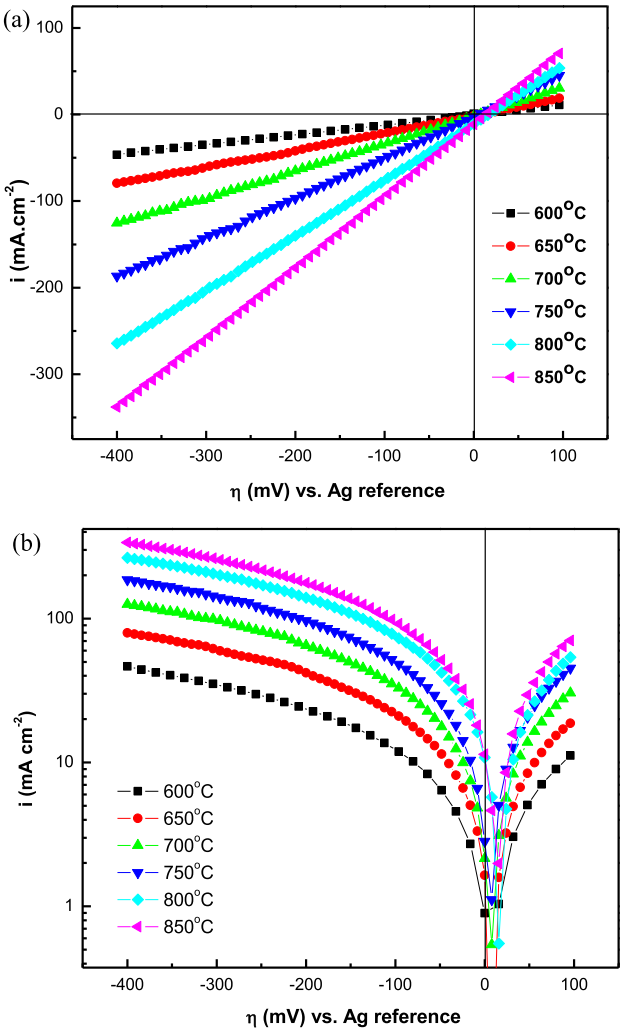

Fig. 5 – (a) The cyclic voltammogram and (b) Tafel plots at 0.5 mVs^{-1} between 100 mV and −400 mV of 70SBSC-30SDC composite cathode on SDC electrolyte over the temperature range of 600–850 °C in air.

$$\text{Log } i = \log i_o + \frac{\alpha nF}{2.3RT}\eta \tag{8}$$

where η is the cathodic polarization, and for the transfer coefficient α, $\alpha = \gamma/\nu + r$ $\beta = 0.5$, where γ, r and β are, respectively, the number of electrons passed before the rate limiting step, the number of electrons passed in the rate limiting step, and the symmetry coefficient, normally assumed to be 0.5 [39]. The i_o values of 70SBSC-30SDC composite cathodes via EIS, LF and HF technique are summarized in Table 3. The i_o value determined by EIS technique is the greatest among measuring techniques. The i_o values measured via various methods can be ranked as EIS > HF > LF. The comparison of i_o values of various cathode determined via EIS technique is listed in Table 4, which indicates that 70SBSC-30SDC revealed a better electrocatalytic activity compared with the other cathodes.

Fig. 6 shows the Arrhenius plots for i_o values collected at 70SBSC-30SDC composite cathode over the operating temperature range of 600–850 °C, using the EIS, LF and HF

Table 3 – The i_o values for the 70SBSC-30SDC composite cathode via EIS, low-field and high-field technique over the temperature range of 600–850 °C.

T (°C)	i_o (mA/cm^2)		
	LF	HF	EIS
600	2.5	6.8	10.9
650	4.1	12.8	36.8
700	6.8	19.5	99.8
750	10.7	30.3	268.8
800	15.3	49.7	543.9
850	20.5	65.2	1008.0

Table 4 – The comparison of i_o values of various cathode via EIS technique.

T (°C)	i_o (mA cm^{-2})				
	SBSC-SDC	LCNC-SDC [40]	LSCF [41]	LSM-YSZ [41]	LSM-YSZ [42]
600	11	0.82	13	0.45	2.40
700	100	4	65	5.80	31
800	544	18			

technique. From the slope of the Arrhenius plots, the overall activation energy (E_a) for the ORR was determined by the following equation.

$$\mathrm{Ln}i_o = \ln K - \frac{E_a}{RT} \quad (9)$$

where K is the pre-exponential constant, which can be calculated from the y-intercept, and E_a is the reaction activation energy. The E_a for the ORR may be related to different cathode preparation methods, the cathode structure, or different cathode compositions. The E_a values determined via EIS, LF and HF techniques were 148.6 kJ mol^{-1}, 69.8 kJ mol^{-1} and 74.2 kJ mol^{-1}, respectively. The linearity of the Arrhenius plots indicates that 70SBSC-30SDC composite cathodes are stable as a function of temperature. Comparing i_o value of 70SBSC-30SDC with the other cathodes, it is suggested that SBSC is a potential cathode for IT-SOFCs due to its highly electrocatalytic activity.

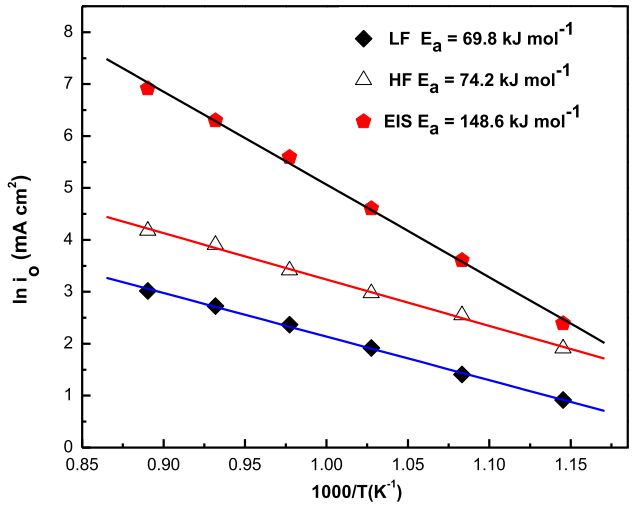

Fig. 6 – Arrhenius plots, $\mathrm{ln}i_o$ versus 1000/T, for 70SBSC-30SDC composite cathode in air. i_o values obtained using EIS, low-field and high-field technique.

Conclusions

This study mainly investigated the bulk diffusion coefficient (D_{chem}) and exchange current density (i_o) of $SmBa_{0.6}Sr_{0.4}Co_2O_{5+\delta}$ for potential applications as a cathode for IT-SOFCs. The oxygen reduction activity of an SOFC cathode is closely related to the oxygen bulk diffusion properties. Through the electrical conductivity relaxation (ECR) test, the values of D_{chem} for SBSC were measured from 1.63×10^{-6} cm^2 s^{-1} of 500 °C to 1.41×10^{-5} cm^2 s^{-1} of 700 °C. The equation of D_{chem} as a function of the operating temperature in the range of 500–700 °C exhibits as follows:

$$D_{chem} = 1.77 \times 10^{-5}\left(-\frac{68.03(\mathrm{kJ\ mol^{-1}})}{RT}\right)(\mathrm{m^2 s^{-1}})$$

From EIS results, it was found that the area specific resistances (ASRs) for SBSC were 5.16, 0.86 and 0.21 Ω cm^2 at 600, 700 and 800 °C, respectively. The activation energies of ORR determined from the slope of Arrhenius plots, $\mathrm{ln}i_o$ versus 1000/T, for EIS, LF and HF techniques were 148.6 kJ mol^{-1}, 69.8 kJ mol^{-1} and 74.2 kJ mol^{-1}, respectively. The SBSC revealed highly electrocatalytic activity comparing with the other cathodes, therefore, it is a potential cathode for IT-SOFCs based on an SDC electrolyte.

Acknowledgments

The authors would like to thank Ministry of Science and Technology of Taiwan for financially supporting this research under Contract no. NSC 102-2113-M-259-004.

REFERENCES

[1] Shao ZP, Haile SM. A high-performance cathode for the next generation of solid oxide fuel cells. Nature 2004;431:170–3.
[2] Zhou W, Shao ZP, Ran R, Jin WQ, Xu NP. A novel efficient oxide electrode for electrocatalytic oxygen reduction at 400–600°C. Chem Commun 2008;44:5791–3.
[3] Liu BW, Zhang Y, Zhang LM. Oxygen reduction mechanism at $Ba_{0.5}Sr_{0.5}Co_{0.8}Fe_{0.2}O_{3-\delta}$ cathode for solid oxide fuel cell. Int J Hydrogen Energy 2009;34:1008–14.
[4] Chen XJ, Chan SH, Khor KA. Simulation of a composite cathode in solid oxide fuel cells. Electrochim Acta 2004;41:1851–61.
[5] Chen D, Shao Z. Surface exchange and bulk diffusion properties of $Ba_{0.5}Sr_{0.5}Co_{0.8}Fe_{0.2}O_{3-\delta}$ mixed conductor. Int J Hydrogen Energy 2011;36:6948–56.
[6] Bucher E, Egger A, Ried P, Sitte W, Holtappels P. Oxygen nonstoichiometry and exchange kinetics of $Ba_{0.5}Sr_{0.5}Co_{0.8}Fe_{0.2}O_{3-\delta}$. Solid State Ion 2008;179:1032–5.
[7] Chen X, Wang S, Yang YL, Smith L, Wu NJ, Kim BI, et al. Electrical conductivity relaxation studies of an epitaxial $La_{0.5}Sr_{0.5}CoO_{3-\delta}$ thin film. Solid State Ion 2002;146:405–13.

[8] Zomorrodian A, Salamati H, Lu ZG, Chen X, Wu NJ, Ignatiev A. Electrical conductivity of epitaxial $La_{0.6}Sr_{0.4}Co_{0.2}Fe_{0.8}O_{3-\delta}$ thin films grown by pulsed laser deposition. Int J Hydrogen Energy 2010;35:12443–8.

[9] Yasuda I, Hikita T. Precise determination of the chemical diffusion coefficient of calcium-doped lanthanum chromites by means of electrical conductivity relaxation. J Electrochem Soc 1994;141:1268–73.

[10] Yasuda I, Hishinuma M. Electrical conductivity and chemical diffusion coefficient of Sr-doped lanthanum chromites. Solid State Ion 1995;80:141–50.

[11] Yasuda I, Hishinuma M. Electrical conductivity and chemical diffusion coefficient of strontium-doped lanthanum manganites. J Solid State Chem 1996;123:382–90.

[12] Brandon NP, Skinner S, Steele BCH. Recent advances in materials for fuel cells. Annu Rev Mater Sci 2003;33:183–213.

[13] Zhou Q, He T, Ji Y. $SmBaCo_2O_{5+\delta}$ double-perovskite structure cathode material for intermediate-temperature solid-oxide fuel cells. J Power Sources 2008;185:754–8.

[14] Chen DJ, Ran R, Zhang K, Wang J, Shao ZP. Intermediate-temperature electrochemical performance of a polycrystalline $PrBaCo_2O_{5+\delta}$ cathode on samarium-doped ceria electrolyte. J Power Sources 2009;188:96–105.

[15] Zhao F, Wang S, Brinkman K, Chen F. Layered perovskite $PrBa_{0.5}Sr_{0.5}Co_2O_{5+\delta}$ as high performance cathode for solid oxide fuel cells using oxide proton-conducting electrolyte. J Power Sources 2010;195:5468–73.

[16] Tarancón A, Burriel M, Santiso J, Skinner SJ, Kilner JA. Advances in layered oxide cathodes for intermediate temperature solid oxide fuel cells. J Mater Chem 2010;20:3799–813.

[17] Lee Y, Kim DY, Choi GM. $GdBaCo_2O_{5+x}$ cathode for anode-supported ceria SOFCs. Solid State Ion 2011;192:527–30.

[18] Frontera C, Caneiro A, Carrillo AE, Oró-Solé J, García-Muñoz JL. Tailoring oxygen content on $PrBaCo_2O_{5+\delta}$ layered cobaltites. Chem Mater 2005;17:5439–45.

[19] Parfitt D, Chroneos A, Tarancón A, Kilner JA. Oxygen ion diffusion in cation ordered/disordered $GdBaCo_2O_{5+\delta}$. J Mater Chem 2011;21:2183–6.

[20] Kim JH, Irvine JTS. Characterization of layered perovskite oxides $NdBa_{1-x}Sr_xCo_2O_{5-\delta}$ ($x = 0$ and 0.5) as cathode materials for IT-SOFC. Int J Hydrogen Energy 2012;37:5920–9.

[21] Xue J, Shen Y, He Y. Performance of double-perovskite $YBa_{0.5}Sr_{0.5}Co_2O_{5-\delta}$ as cathode material for intermediate-temperature solid oxide fuel cells. Int J Hydrogen Energy 2011;36:6894–8.

[22] Fu YP, Wen SB, Lu CH. Preparation and characterization of samaria-doped ceria electrolyte materials for solid oxide fuel cells. J Am Ceram Soc 2008;91:127–31.

[23] Adler SB, Henderson BT, Wilson MA, Taylor DM, Richards RE. Reference electrode placement and seals in electrochemical oxygen generators. Solid State Ion 2000;134:35–42.

[24] Winkler J, Hendriksen PV, Bonanos N, Mogensen M. Geometric requirements of solid electrolyte cells with a reference electrode. J Electrochem Soc 1998;145:1184–92.

[25] Chan SH, Chen XJ, Khor KA. Reliability and accuracy of measured overpotential in a three-electrode fuel cell system. J Appl Electrochem 2001;31:1163–70.

[26] Ding H, Xue X, Liu X, Meng G. High performance layered $SmBa_{0.5}Sr_{0.5}Co_2O_{5+\delta}$ cathode for intermediate-temperature solid oxide fuel cells. J Power Sources 2009;194:815–7.

[27] Jun A, Kim J, Shin J, Kim G. Optimization of Sr content in layered $SmBa_{1-x}Sr_xCo_2O_{5-\delta}$ perovskite cathodes for intermediate-temperature solid oxide fuel cells. Int J Hydrogen Energy 2012;37:18381–8.

[28] Dunwald H, Wagner C. Measurement of diffusion rate in the process of dissolving gases in solid phases. Z Phys Chem B 1934;24:53–8.

[29] Elshof JE, Lankhorst MHR, Bouwmeester HJM. Oxygen exchange and diffusion coefficients of strontium-doped lanthanum ferrites by electrical conductivity relaxation. J Electrochem Soc 1997;144:1060–7.

[30] Leng Y, Chan SH, Liu Q. Development of LSCF-GDC composite cathodes for low-temperature solid oxide fuel cells with thin film GDC electrolyte. Int J Hydrogen Energy 2008;33:3808–17.

[31] Co AC, Xia SJ, Birss VI. A kinetic study of the oxygen reduction reaction at $LaSrMnO_3$-YSZ composite electrodes. J Electrochem Soc 2005;152:570–6.

[32] Zhou W, Ran R, Shao Z, Cai R, Jin W, Xu N. Electrochemical performance of silver-modified $Ba_{0.5}Sr_{0.5}Co_{0.8}Fe_{0.2}O_{3-\delta}$ cathodes prepared via electroless deposition. Electrochim Acta 2008;53:4370–80.

[33] Adler SB. Limitations of charge-transfer models for mixed-conducting oxygen electrodes. Solid State Ion 2000;135:603–12.

[34] Qiang F, Sun KN, Zhang NQ, Zhu XD, Le SR, Zhou DR. Characterization of electrical properties of GDC doped A-site deficient LSCF based composite cathode using impedance spectroscopy. J Power Sources 2007;168:338–45.

[35] Ding X, Kong X, Wu H, Zhu Y, Tang J, Zhong Y. $SmBa_{0.5}Sr_{0.5}Cu_2O_{5-\delta}$ and $SmBa_{0.5}Sr_{0.5}CuFeO_{5+\delta}$ layered perovskite oxides as cathodes for IT-SOFCs. Int J Hydrogen Energy 2012;37:2546–51.

[36] Adler SB. Factors governing oxygen reduction in solid oxide fuel cell cathodes. Chem Rev 2004;104:4791–843.

[37] Piao J, Sun K, Zhang N, Chen X, Xu S, Zhou D. Preparation and characterization of $Pr_{1-x}Sr_xFeO_3$ cathode material for intermediate temperature solid oxide fuel cells. J Power Sources 2007;172:633–40.

[38] Liu J, Co AC, Paulson B, Birss VI. Oxygen reduction at sol-gel derived $La_{0.8}Sr_{0.2}Co_{0.8}Fe_{0.2}O_3$ cathode. Solid State Ion 2006;177:377–87.

[39] Bockris JOM, Reddy AKN. Modern electrochemistry: an introduction to an interdisciplinary area. New York: Plenum Publishing Corporation; 1977.

[40] Fu YP, Tsai FY. Composite cathodes of $La_{0.9}Ca_{0.1}Ni_{0.5}Co_{0.5}O_3$-$Ce_{0.8}Sm_{0.2}O_{1.9}$ for solid oxide fuel cells. Ceram Int 2011;37:231–9.

[41] Xia CR, Rauch W, Chen FL, Liu ML. $Sm_{0.5}Sr_{0.5}CoO_3$ cathodes for low-temperature SOFCs. Solid State Ion 2002;149:11–9.

[42] Hwang HJ, Moon JW, Moon J. Removal of nitric oxide (NO) by perovskite-type composite catalytic thick film, $La_{0.6}Sr_{0.4}Co_{0.2}Fe_{0.8}O_{3-\delta}$ and gadolinia-doped ceria electrolyte, $Gd_{0.2}Ce_{0.8}O_2$. J Am Ceram Soc 2005;88:79–84.